Concrete Resistivity: Interim Observations Due to Potential Aggregate Impacts

White Paper
December 2024

Sponsored by
Federal Highway Administration
Office of Preconstruction, Construction, and Pavements
(Part of Cooperative Agreement 693JJ31950004)

IOWA STATE UNIVERSITY
Institute for Transportation

National Concrete Pavement Technology Center
Tech Center

About the CP Tech Center

The mission of the National Concrete Pavement Technology Center (CP Tech Center) at Iowa State University is to unite key transportation stakeholders around the central goal of developing and implementing innovative technology and best practices for sustainable concrete pavement construction and maintenance.

About the Institute for Transportation

The mission of the Institute for Transportation (InTrans) at Iowa State University is to save lives and improve economic vitality through discovery, research innovation, outreach, and the implementation of bold ideas.

Iowa State University Nondiscrimination Statement

Iowa State University does not discriminate on the basis of race, color, age, ethnicity, religion, national origin, pregnancy, sexual orientation, gender identity, genetic information, sex, marital status, disability, or status as a US veteran. Inquiries regarding nondiscrimination policies may be directed to the Office of Equal Opportunity, 3410 Beardshear Hall, 515 Morrill Road, Ames, Iowa 50011, telephone: 515-294-7612, hotline: 515-294-1222, email: eooffice@iastate.edu.

Notice

This document is disseminated under the sponsorship of the U.S. Department of Transportation in the interest of information exchange. The U.S. Government assumes no liability for the use of the information contained in this document.

The U.S. Government does not endorse products or manufacturers. Trademarks or manufacturers' names appear in this report only because they are considered essential to the objective of the document. They are included for informational purposes only and are not intended to reflect a preference, approval, or endorsement of any one product or entity.

Nonbinding Contents

The contents of this document do not have the force and effect of law and are not meant to bind the public in any way. This document is intended only to provide clarity to the public regarding existing requirements under the law or agency policies. However, compliance with applicable statutes or regulations cited in this document is required.

Quality Assurance Statement

The Federal Highway Administration (FHWA) provides high-quality information to serve Government, industry, and the public in a manner that promotes public understanding. Standards and policies are used to ensure and maximize the quality, objectivity, utility, and integrity of its information. FHWA periodically reviews quality issues and adjusts its programs and processes to ensure continuous quality improvement.

Technical Report Documentation Page

1. Report No.	2. Government Accession No.	3. Recipient's Catalog No.	
4. Title and Subtitle Concrete Resistivity: Interim Observations Due to Potential Aggregate Impacts		**5. Report Date** December 2024 **6. Performing Organization Code**	
7. Author(s) Jason Weiss and Burkan Isgor		**8. Performing Organization Report No.**	
9. Performing Organization Name and Address National Concrete Pavement Technology Center Iowa State University 2711 South Loop Drive, Suite 4700 Ames, IA 50010-8664		**10. Work Unit No. (TRAIS)** **11. Contract or Grant No.** Part of Cooperative Agreement 693JJ31950004, Advancing Concrete Pavement Technology Solutions	
12. Sponsoring Organization Name and Address Office of Preconstruction, Construction, and Pavements Federal Highway Administration 1200 New Jersey Avenue, SE Washington, DC 20590		**13. Type of Report and Period Covered** White Paper **14. Sponsoring Agency Code**	

15. Supplementary Notes

Visit https://cptechcenter.org/ for color pdfs of this and other publications. The FHWA Contracting Officer was Robert Spragg.

16. Abstract

The electrical properties of concrete are often used as a surrogate test method to assess fluid transport in concrete primarily because resistivity can be measured rapidly and economically. While resistivity has been measured for nearly a century, the recent rise in handheld, battery-operated testing tools coupled with the desire to quantify the transport performance of concrete has caused a sudden spike in interest in resistivity measurement as a quality control or quality acceptance tool. Standards have been developed (AASHTO T 358, AASHTO T 402, ASTM C1876) with an emphasis on the role of sample conditioning. As a result, many state highway agencies (SHAs) have explored the use of resistivity. Some SHAs have reported that the use of certain aggregates tended to reduce the resistivity values when compared with concrete made using the same matrix but different aggregates.

This white paper examines one fundamental assumption of the resistivity testing, i.e., that the aggregate is resistive or nonconductive. It explores the implications if the aggregate is conductive using both an analytical and finite element approach to determining the impact of aggregate with a lower resistivity and discusses a procedure to account for aggregate resistivity. An experimental procedure is proposed to account for aggregate resistivity. In addition, the impact of conductive aggregate size and the probe spacing used for surface resistivity measurements is discussed.

17. Key Words	18. Distribution Statement		
aggregate resistivity—fluid transport—surface resistivity—transport properties	No restrictions.		
19. Security Classification (of this report)	**20. Security Classification (of this page)**	**21. No. of Pages**	**22. Price**
Unclassified.	Unclassified.	30	NA

Form DOT F 1700.7 (8-72) **Reproduction of completed page authorized**

CONCRETE RESISTIVITY: INTERIM OBSERVATIONS DUE TO POTENTIAL AGGREGATE IMPACTS

White Paper
December 2024

Authors
Jason Weiss and Burkan Isgor

Sponsored by
Federal Highway Administration
(Part of Cooperative Agreement 693JJ31950004,
Advancing Concrete Pavement Technology Solutions)

A white paper from
National Concrete Pavement Technology Center
Iowa State University
2711 South Loop Drive, Suite 4700
Ames, IA 50010-8664
Phone: 515-294-8103 / Fax: 515-294-0467
https://cptechcenter.org

TABLE OF CONTENTS

LIST OF FIGURES

LIST OF TABLES

ACKNOWLEDGMENTS

The authors would like to thank the Federal Highway Administration (FHWA) for sponsoring this research as part of Cooperative Agreement 693JJ31950004, Advancing Concrete Pavement Technology Solutions, Work Order 2.

Note that this work contains a collection of thoughts assembled in 2011 during the first author's sabbatical at the National Institute of Standards and Technology (NIST), during which he had many fruitful discussions with Dale Bentz, Ken Snyder, Ed Garboczi, and Jeff Bullard. This work was continued when the first author returned to Purdue; however, the work was halted when it was determined that the influence of lightweight aggregate (LWA) sand in internally cured concrete was likely very small.

The data series using LWA steel aggregate was measured by Javier Castro while the first author was at Purdue. The data from Iowa were provided by Todd Hanson (Iowa Department of Transportation). The authors also gratefully acknowledge discussions with John Staton while he was at the Michigan Department of Transportation. Assembling the summary of this work into a white paper was supported in a project from FHWA through the National Concrete Pavement Technology Center at Iowa State University to determine the potential impact of conductive aggregate in November and December 2024.

EXECUTIVE SUMMARY

The electrical properties of concrete are often used as a surrogate test method to assess fluid transport in concrete primarily because resistivity can be measured rapidly and economically. While resistivity has been measured for nearly a century, the recent rise in handheld, battery-operated testing tools coupled with the desire to quantify the transport performance of concrete has caused a sudden spike in interest in resistivity measurement as a quality control or quality acceptance tool. Standards have been developed (AASHTO T 358, AASHTO T 402, ASTM C1876) with an emphasis on the role of sample conditioning. As a result, many state highway agencies (SHAs) have explored the use of resistivity. Some SHAs have reported that the use of certain aggregates tended to reduce the resistivity values when compared with concrete made using the same matrix but different aggregates.

This white paper examines one fundamental assumption of the resistivity testing, i.e., that the aggregate is resistive or nonconductive. It explores the implications if the aggregate is conductive using both an analytical and finite element approach to determining the impact of aggregate with a lower resistivity and discusses a procedure to account for aggregate resistivity. An experimental procedure is proposed to account for aggregate resistivity. In addition, the impact of conductive aggregate size and the probe spacing used for surface resistivity measurements is discussed.

1.0 CONCERNS REGARDING RESISTIVITY MEASURED USING SPECIFIC AGGREGATES

A few concrete producers have expressed concern with reaching the resistivity values when certain aggregates are used. For example, recent research in Iowa noticed a sensitivity to coarse-grained dolomites in north central Iowa (Shankaramurthy et al. 2021). Similar questions have been raised in Michigan (J. Staton, personal communication, 2020) and New York (H. Steffek, personal communication, 2024). Earlier work examined the use of fine lightweight aggregate (LWA) for internally cured concrete.

The intent of this white paper is to examine the role that aggregate conductivity may have and whether concrete is sensitive to the resistivity of the aggregate to ultimately identify a procedure that may be used as a potential method to quantify this behavior.

2.0 BACKGROUND

The electrical properties of concrete have been used as a surrogate test to assess fluid transport in concrete, as resistivity can be measured rapidly and economically (Spragg et al. 2011). One important fundamental assumption that is made in the measurement of these properties is that the aggregate typically has a resistivity that is several orders of magnitude greater than that of the paste (Rajabipour and Weiss 2006). This is provided as background to understand the implications that a less resistive (i.e., more electrically conductive) aggregate may have.

2.1 Fundamental Assumption on Measuring the Electrical Properties of Concrete

Concrete consists of liquid, solid, and vapor phases, as shown schematically in Figure 1.

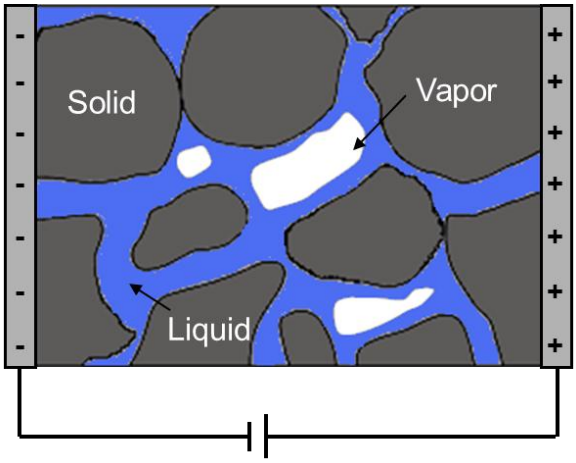

Figure 1. Schematic illustration of the three phases in concrete

The vapor-filled spaces are generally air-filled pockets containing water vapor. Typically, the resistivity of the vapor phase is on the order of 10^{14} Ω-m (a quadrillion) (Aplin 2005). The solid

phases consist of aggregate and "dried" hydration products (calcium silicate hydrate [CSH] and calcium hydroxide [CH]) and have a resistivity on the order of 10^8 Ω-m (a billion) (Aplin 2005). The fluid phase is the pore solution with a resistivity on the order of 0.05 to 1 Ω-m (Aplin 2005). Clearly, these resistivities span a wide range of magnitudes.

The constituents of concrete can be considered as resistors, and as a first approximation it can be assumed that roughly 15% of the system is fluid and 10% is vapor. While a simple parallel model does not consider the intricacies of phase connectivity, its application can provide valuable insight into the electrical response of concrete. Concrete made using these assumptions would have a resistivity of between 0.15 and 2.85 Ω-m, and nearly all the conduction would occur through the liquid phase. This has further been demonstrated with experiments where the fluid is replaced with vapor due to drying (Schießl et al. 2000) or when the concrete is frozen (Farnam et al. 2015) and a portion of the fluid becomes ice, which has a high resistivity (the resistivity of sea ice is 10 kΩ-m [Reynolds and Paren 1984]).

As a result, a modified parallel law (or Archie's law) is often used to describe the transport in concrete assuming that the fluid phase is the only conductive phase, as shown in equation (1) (written in terms of conductivity in 1a and resistivity in 1b) (Weiss et al. 2013).

$$\sigma = \sigma_s \emptyset \beta = \frac{\sigma_s}{F} \tag{1a}$$

where σ is the concrete conductivity (S/m), σ_s is the pore solution conductivity (S/m), ϕ is the fluid filled porosity (unitless volume fraction ratio), and β is the connectivity (unitless ratio).

$$\rho = \rho_s \frac{1}{\emptyset \beta} = \rho_s F \tag{1b}$$

where ρ is the concrete resistivity (Ω-m) and ρ_s is the pore solution resistivity (Ω-m).

2.2 The Role of Saturation

Equation (1) can be rewritten in terms of the porosity of the concrete, assuming that it is not fully saturated, using equation (2) (Weiss et al. 2013).

$$\frac{\sigma_P}{\sigma_o} = S \varphi \beta = S \frac{1}{F} \tag{2a}$$

$$\frac{\rho_P}{\rho_o} = \frac{1}{S \varphi \beta} = \frac{1}{S} F \tag{2b}$$

where S is a saturation function. It is logical that S should be dependent on either moisture content, and this has been described using a Power Law (Weiss et al. 2013) as well as a Gel-Capillary-Air (GCA) model (Barrett et al. 2013). Previous work has also typically assumed that the only portion of the system susceptible to moisture-related effects is the paste.

Aggregates generally have relatively low porosity (i.e., <3%) and the pores are often disconnected, resulting in the aggregate remaining more resistive than the paste (by at least an order of magnitude) and therefore having a minimal impact on the resistivity of the concrete. Further, the pores in aggregate are often larger than the pores in pastes, causing them to dry more rapidly. However, there are cases where the aggregate can be more porous and conductive.

A series of LWAs (with an average 24-hour absorption of 8%) were tested (nominally 20 mm x 17 mm x 10 mm) at five different relative humidities (100%, 97.5%, 94.2%, 86%, and 0% obtained using saturated salt solutions). Figure 2a illustrates a desorption isotherm for the LWA. As depicted in Figure 2b, the conductivity of the LWA changes depending on the degree of saturation of the aggregate (based on unpublished data from J. Weiss, 2012). Water is more easily lost from the LWA at higher relative humidities due to the larger pore sizes.

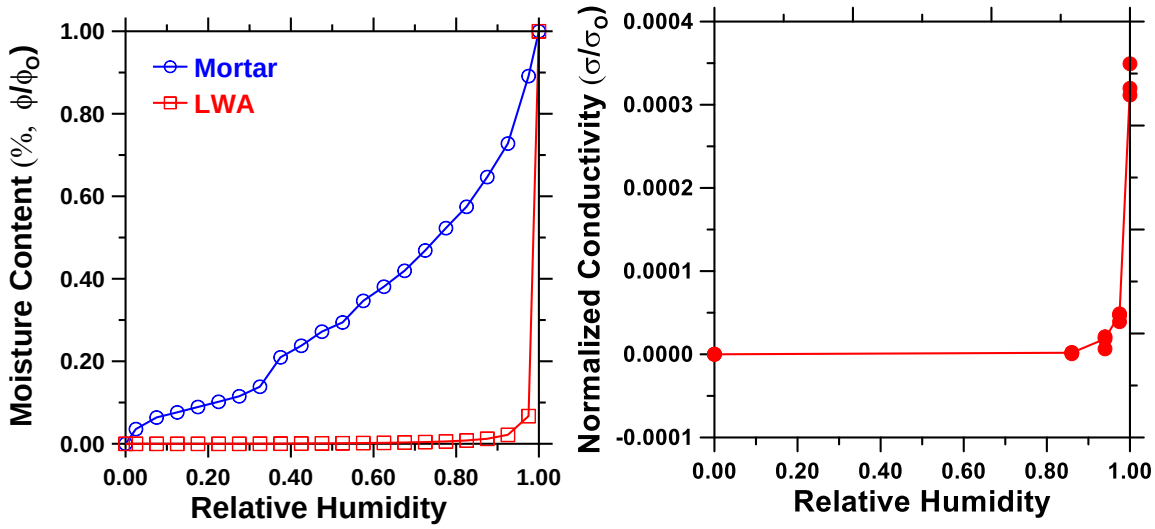

Figure 2. Desorption spectra for mortar and LWA

Similar observations have been made for siltstone (Rajabipour and Weiss 2006) and limestone aggregate (J. Weiss, unpublished data, 2012), where the porosity of these aggregates results in the aggregates having measurable conductivity.

3.0 ANALYTICAL SOLUTION FOR CEMENTITIOUS COMPOSITES WITH CONDUCTIVE AGGREGATES

To explicitly relate the resistivity of concrete when conductive aggregate is added to paste or mortar, composite theory is used. In the late 1870s, Maxwell developed an approximation for cases where spherical inclusions of a known resistivity (1/conductivity) are added to a matrix with a known resistivity. This can be a paste or mortar. The resistivity of the spherical inclusions can be considered along with the resistivity of the matrix to compute the effective composite resistivity (the resistivity of the concrete, 1/conductivity of the concrete), as shown in equation (3).

$$\frac{\sigma_e-\sigma_P}{\sigma_e+\sigma_P(d-1)} = \emptyset_P\left[\frac{\sigma_A-\sigma_P}{\sigma_A+\sigma_P(d-1)}\right] \quad (3)$$

where σ_A is the conductivity of the aggregate, σ_P is the conductivity of the paste, ϕ_A is the volume fraction of the aggregate, and d is the dimensional characterization number (d is assumed to be 3 for the discussion in this paper, though it could be varied as desired).

This approach has been shown to work both for dilute and non-dilute systems (Tarquato 2001). Rearranging this equation (and setting d = 3) enables the following expression to be developed, the results of which are shown in Figure 3a.

$$\frac{\sigma_e}{\sigma_P} = \frac{1+2\emptyset_A\left[\frac{\frac{\sigma_A}{\sigma_P}-1}{\frac{\sigma_A}{\sigma_P}+2}\right]}{1-\emptyset_A\left[\frac{\frac{\sigma_A}{\sigma_P}-1}{\frac{\sigma_A}{\sigma_P}+2}\right]} \quad (4a)$$

$$\frac{\rho_{conc}}{\rho_{mortar}} = \frac{1-\emptyset_A\left[\frac{\frac{\rho_{mortar}}{\rho_{agg}}-1}{\frac{\rho_{mortar}}{\rho_{agg}}+2}\right]}{1+2\emptyset_A\left[\frac{\frac{\rho_{mortar}}{\rho_{agg}}-1}{\frac{\rho_{mortar}}{\rho_{agg}}+2}\right]} \quad (4b)$$

If the aggregate is nonconductive (i.e., $\sigma_A/\sigma_P = 0$), the effective composite conductivity decreases, and if the aggregate conductivity is greater than the paste conductivity ($\sigma_A/\sigma_P > 1$), the overall effective composite conductivity (i.e., the concrete conductivity) increases (Figure 3a). This indicates that the conductivity of the aggregate could play a significant role in influencing the overall conductivity of the concrete sample. Figure 3b illustrates that at very low conductivities ($\sigma_A/\sigma_P < 0.01$, i.e., high resistivities $\rho_A/\rho_P > 100$), the aggregate can be assumed to be asymptotic and relatively nonconducting, while at relatively high conductivities ($\sigma_A/\sigma_P > 100$, i.e., low resistivities $\rho_A/\rho_P < 0.01$), the behavior converges toward an asymptote as well that is similar to considering $\sigma_A/\sigma_P = \infty$.

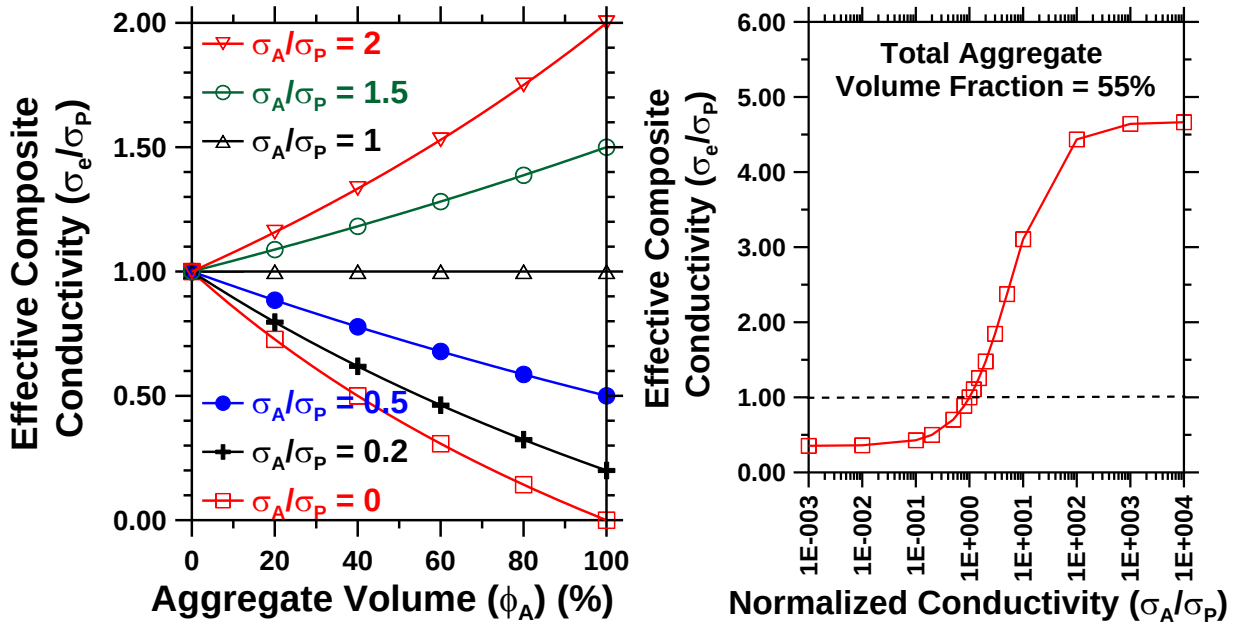

Figure 3. Illustration of the role of aggregate conductivity on the composite conductivity (i.e., the mortar or concrete conductivity

It is also interesting to note that equation (2) for nonconductive (i.e., highly resistive) aggregate can be rewritten as shown in equation (5). (Here the porosity, connectivity, saturation, and formation factor all refer to that of the paste.)

$$\frac{\sigma_e}{\sigma_o} = S\varphi\beta\left[\frac{1-\emptyset_A}{1+\frac{1}{2}\emptyset_A}\right] = S\frac{1}{F}\left[\frac{1-\emptyset_A}{1+\frac{1}{2}\emptyset_A}\right] \tag{5a}$$

$$\frac{\rho_P}{\rho_o} = \frac{1}{S\varphi\beta}\left[\frac{1+\frac{1}{2}\emptyset_A}{1-\emptyset_A}\right] = \frac{1}{S}F\left[\frac{1+\frac{1}{2}\emptyset_A}{1-\emptyset_A}\right] \tag{5b}$$

Equation (4) considers that all of the aggregates have the same conductivity, which may not be the case for some concretes. As such, equation (6) can be used for different types of spherical inclusions:

$$\frac{\sigma_e-\sigma_P}{\sigma_e+\sigma_P(d-1)} = \sum_{j=1}^{M}\emptyset j\left[\frac{\sigma_j-\sigma_P}{\sigma_j+\sigma_P(d-1)}\right] \tag{6}$$

where the aggregate phases are listed as 1 to j.

Equation (7) can be written by assuming that there is a conductive aggregate (CA) phase and nonconductive aggregate (NCA) phase to yield equation (7).

$$\frac{\sigma_e}{\sigma_P} = \frac{1-\emptyset_{NCA}+2\emptyset_{CA}\left[\frac{\frac{\sigma_{CA}}{\sigma_P}-1}{\frac{\sigma_{CA}}{\sigma_P}+2}\right]}{1+\frac{1}{2}\emptyset_{NCA}-\emptyset_{CA}\left[\frac{\frac{\sigma_{CA}}{\sigma_P}-1}{\frac{\sigma_{CA}}{\sigma_P}+2}\right]} \quad (7)$$

where ϕ_{CA} is the volume fraction of conductive aggregate, ϕ_{NCA} is the volume fraction of nonconductive aggregate, σ_{CA} is the conductivity of conductive aggregate, and σ_{NCA} is the conductivity of nonconductive aggregate. It is also convenient to normalize the conductivity of the concrete by the conductivity of the paste (or mortar) and to normalize the conductivity of the aggregate by the conductivity of the paste (or mortar) to help non-dimensionalize the problem.

Figure 4 shows the normalized effective conductivity for concrete with conductive and nonconductive aggregate (equation 7) as a function of the volume fraction of conductive aggregate if the total volume of aggregate remains constant. When only a nonconductive aggregate is used, the normalized effective conductivity is one, as may be expected. As the conductivity of the aggregate increases, the normalized effective conductivity begins to increase.

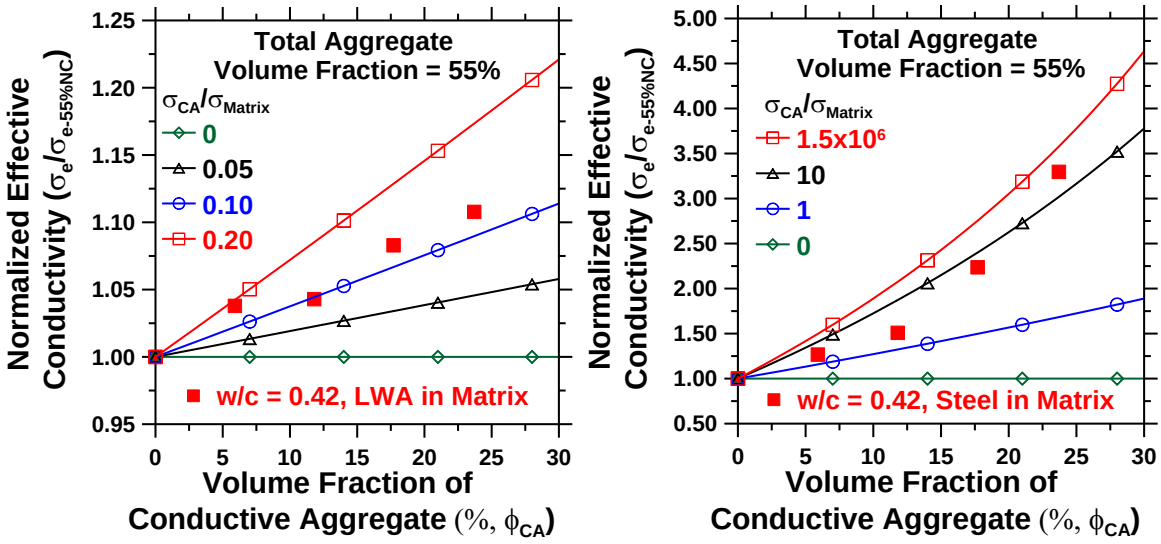

Based on unpublished data from J. Weiss and J. Castro, 2012

Figure 4. Illustration of the influence of conductive aggregate on the effective conductivity of the concrete: (a) moderately conductive aggregate and (b) highly conductive aggregate

To provide a comparison between equation (7) and some experimentally measured data, two experimental series were also added to this graph. The first experimental series considers a mortar with a water-to-cement (w/c) ratio of 0.42 with prewetted LWA (Figure 4a), and the second experimental series considers a mortar with a w/c ratio of 0.42 and spherical stainless steel aggregates (Figure 4b).

It can be noticed that in both cases the conductivity of the cementitious composite (i.e., mortar or concrete) increased with the use of the conductive aggregate. The prewetted LWA was fitted to determine that the σ_{CA}/σ_P is 0.13 at the age of testing, while it was determined that the stainless steel aggregate has a σ_{CA}/σ_P of 6. At this point, it should be noted that the conductivity of the stainless steel aggregate is less than would be expected from theory; however, it is important to remember that as the conductivity of the aggregate increases, it begins to approach an asymptotic value, as illustrated in Figure 3.

Figure 5 shows that the conductivity of the aggregate can be influential on the overall conductivity of the concrete composite.

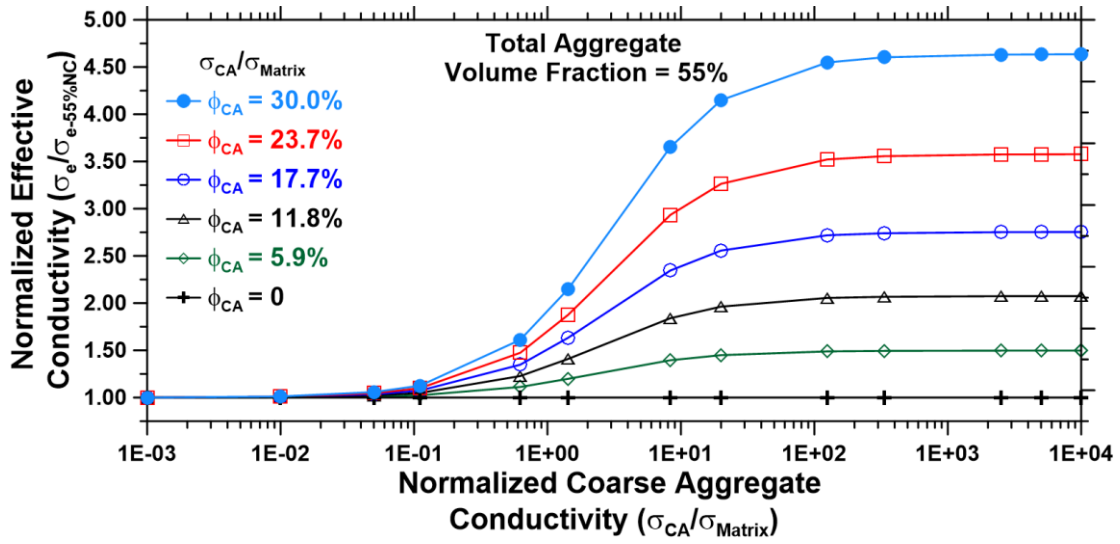

(a)

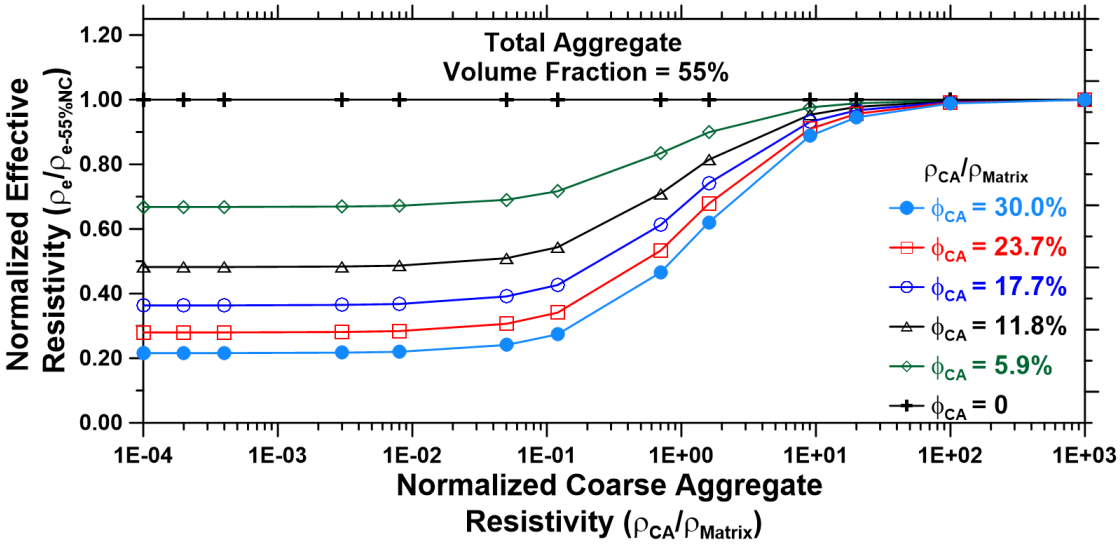

(b)

Figure 5. Influence of (a) aggregate conductivity and (b) aggregate resistivity on the overall measured concrete resistivity

It appears that once the aggregate has a conductivity above a certain threshold (e.g., $\sigma_{CA}/\sigma_P > 0.01$), the conductivity of the aggregate should be considered because it begins to have a measurable impact on the overall conductivity. Similarly, once the conductivity becomes high (e.g., $\sigma_{CA}/\sigma_P > 100$), it may be reasonable to assume that the aggregate is sufficiently conductive. Figure 5b shows the same data in terms of resistivity.

Maxwell's equation has been used to demonstrate that the conductivity (or resistivity) of the aggregate may be important to changing the conductivity (or resistivity) of the concrete composite. This was confirmed experimentally for both concrete with prewetted LWA and concrete with stainless steel aggregates. While Maxwell's approach is very powerful, it should be noted that there are a few limitations. First, this approach considers that the aggregate and paste are two distinct phases, and it does not consider any interfacial transition zone. Second, it does not consider particle shape (other than spherical) or size (though this is seen in some composites). Third, it does not consider the influence of aggregate interaction.

A series of concretes (and a mortar) were made in Iowa using different limestone aggregates (Figure 6). The limestone aggregates had a porosity from 0.7% to 6.8%. The w/c ratio of these systems was 0.40, and equal volumes of fine and coarse aggregate were used (33.7%). The resistivity of the cores of the 0.7% and 6.8% limestone aggregates were soaked in a pore solution, and their resistivities were measured to be approximately 70 and 700 kohm-cm during the first day. The experimental data are well bounded by the Maxwell predictions. The normalized resistivity of these aggregates to mortar is between 0.1 and 208, covering a wide range of the variation shown in Figure 6.

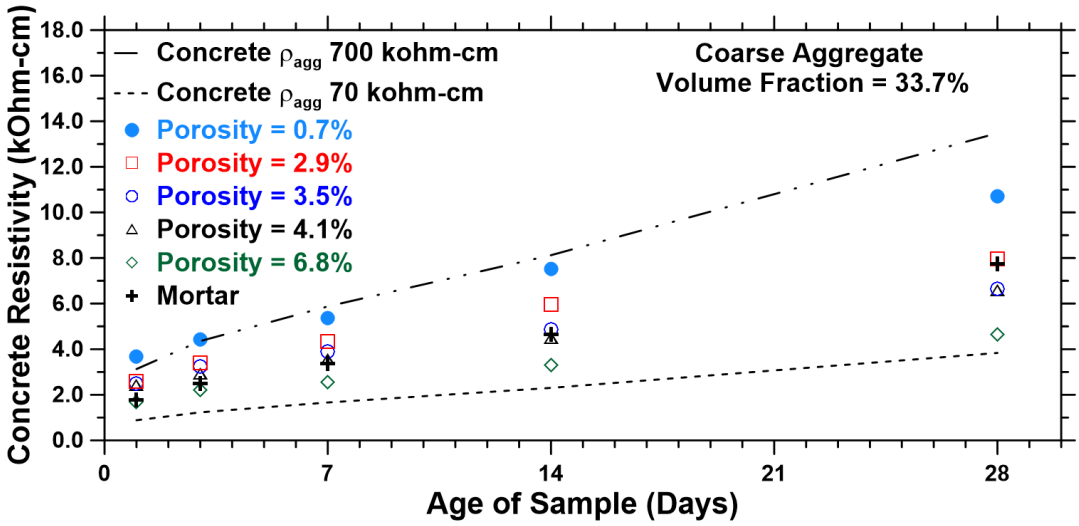

Figure 6. Role of aggregate on the resistivity of concrete: comparison of measurements made in Shankaramurthy et al. 2021 and predictions based on Maxwell's model

The discussion up to this point has not directly considered how the aggregate can influence the properties of the matrix over time. First, as water leaves the aggregate, the aggregate becomes less conductive. This implies that the aggregate may be conductive immediately after casting and

become increasingly less conductive until it effectively "switches off" during the life of the concrete. Second, especially with LWA, the LWA provides water to the matrix that increases the hydration of the cement paste, thereby reducing the conductivity of the paste phase. Third, the water from the aggregate may have a slight impact on the conductivity of the pore solution. Fourth, the aggregate can change the saturation level that can be experienced in the concrete when compared with the conventional concrete at the same age. Finally, it has been shown that the interfacial transition zone around the aggregate may differ from that around a conventional aggregate. It should also be noted that this discussion has only considered the impact of conductive aggregates on electrical properties; however, further examination is needed to assess the impact of these aggregates on ionic transport. To better understand the potential impact of each of these factors, a full investigation should be conducted.

4.0 COMPUTATIONAL SIMULATIONS FOR CONDUCTIVE AGGREGATE

The effect of conductive aggregates on concrete resistivity was studied using the finite element method. Two types of simulations were performed for modeling bulk and surface resistivity. In both cases, the computational process involved the solution of the governing Laplace's equation for electrical potentials, as given in equation (8), using the appropriate boundary conditions, and obtaining the resistivity from the calculated potentials and applied current. The governing equation of the problem can be written as follows (Munn and Devereux 1991):

$$\nabla\left(\frac{1}{\rho}\nabla \mathrm{V}\right) = 0 \tag{8}$$

where ρ is the electrical resistivity (ohm-m) and V (volt) is the electrical potential.

4.1 Bulk Resistivity Simulations

To solve for the bulk resistivity of concrete, the simulations were performed in the cylindrical domain, representing a standard concrete cylinder with a 100 mm diameter and a 200 mm height, as shown in Figure 7a. The domain was discretized using three-dimensional tetragonal Lagrangian elements, as shown in Figure 7b.

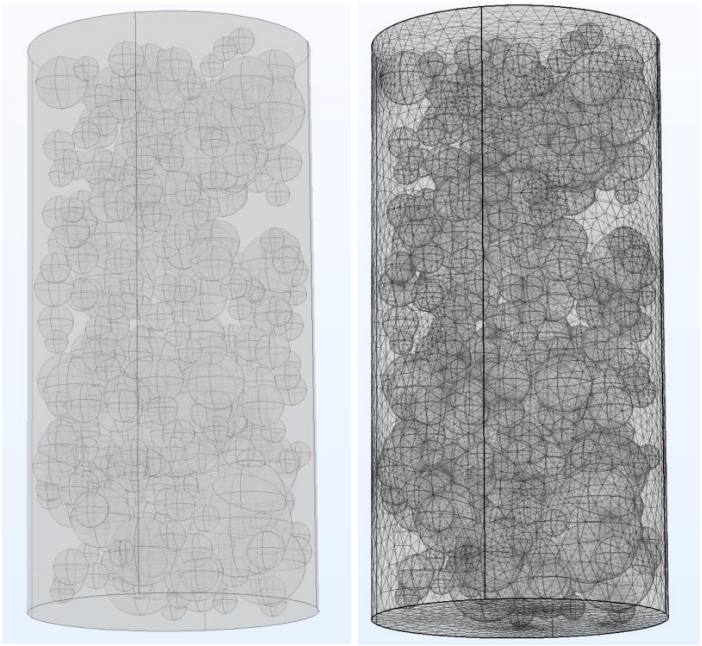

(a) (b)

Figure 7. Standard concrete cylinder with a diameter of 100 mm and a height of 200 mm for bulk resistivity simulations: (a) cylindrical domain containing conductive coarse aggregates and (b) example discretized domain used in the finite element analysis

These simulations followed the typical bulk resistivity measurement for cylindrical samples, where metallic plates are placed at the top and bottom surfaces and the potential difference between the surfaces is measured after a constant current application between the plates. Conductive coarse aggregates were simulated as spheres with a resistivity defined as $\rho_{aggregate}$. The remaining space was assumed to be mortar with a different resistivity from that of the conductive coarse aggregates, defined as ρ_{mortar}. Since the metallic plates (electrodes) at both ends were significantly larger than the coarse aggregates, the particle size distribution or the maximum aggregate size were not expected to affect the resistivity results significantly. However, for simulation purposes, a typical coarse aggregate gradation was used with a maximum aggregate size of 1 in. (25 mm).

A no-flux boundary condition was defined on the sides of the cylinder. From the top plate, a constant current of 1 A was applied. With these boundary conditions, the governing equation given in equation (8) was solved for the electrical potential distribution within the domain. The potential difference between the top and bottom surfaces of the cylinder (ΔV) was calculated, and the bulk resistivity of the cylinder, ρ_b (ohm-m) was solved by Ohm's Law as follows:

$$\rho_b = \frac{\Delta \mathrm{V}}{1[A]} \frac{S}{L} \tag{9}$$

where S is the surface area of the cylinder (m^2) and L is the length of the cylinder (m). The ratio of surface area to length (S/L) is 0.03927 m for the standard cylinder used in the simulations.

The analysis parameters involved the conductive coarse aggregate volume fraction (which varied from 0.1 to 0.4) and the conductive aggregate-to-mortar resistivity ratio (0.25 to 100). Figure 8 shows the computed bulk concrete resistivities for two mortar resistivities: 40 ohm-m (Figure 8a) and 80 ohm-m (Figure 8b). The simulations confirm that bulk concrete resistivity is a function of the conductive aggregate volume fraction and the ratio of the conductive aggregate resistivity to the coarse aggregate resistivity.

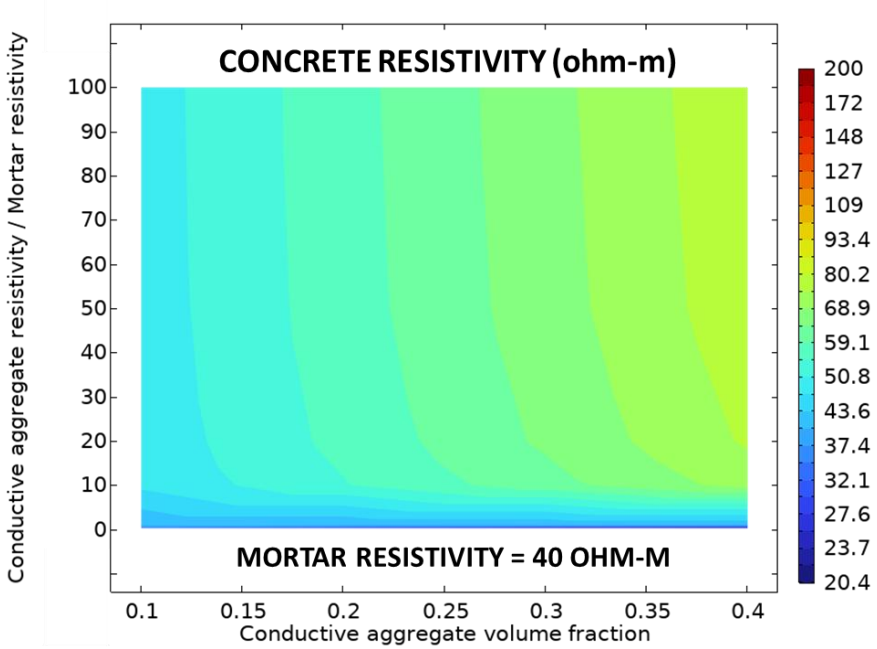

(a)

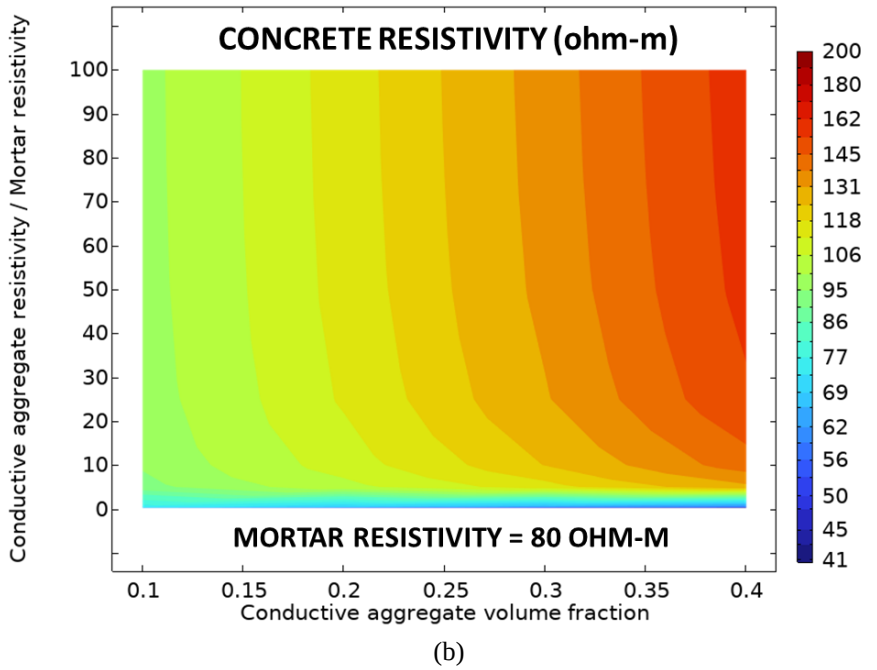

(b)

Figure 8. Computed bulk concrete resistivities for (a) 40 ohm-m mortar and (b) 80 ohm-m mortar

Figure 9 shows the computed concrete resistivities normalized with mortar resistivity.

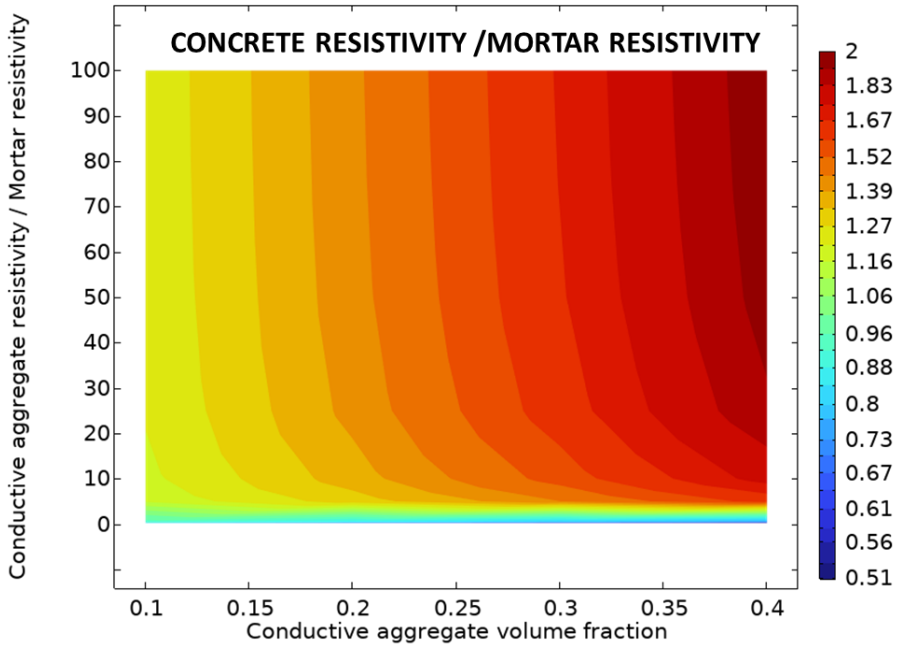

Figure 9. Computed bulk concrete resistivities normalized with mortar resistivity

4.2 Surface Resistivity Simulations

To solve for the surface resistivity of concrete, the simulations were performed in the prismatic domain, with a square planar cross section (450 mm x 450 mm) and a height of 175 mm, as shown in Figure 10. These dimensions were selected after preliminary simulations as the smallest domain size that was large enough to eliminate the errors associated with the geometry of the domain. As in the case of the bulk resistivity simulations, the domain was discretized using three-dimensional tetragonal Lagrangian elements.

The Wenner probe configuration includes four electrodes that are aligned on a straight line at equal distances from each other (i.e., probe spacing, a), as shown in Figure 10. No-flux boundary conditions were defined for the side surfaces of the prism and for the top surface other than the parts under the Wenner probe electrodes. In this configuration, the two outer electrodes are used to impose an electrical current (I = 1 A), whereas the inner electrodes are used to measure the resulting electrical potential difference at two locations (ΔV). Assuming that the measurement domain is semi-infinite, electrical resistivity using the Wenner probe can be calculated via equation (10):

$$\rho_s = 2\Pi a \frac{\Delta V}{1[A]} \tag{10}$$

The surface resistivity simulations were performed to study the effect of conductive coarse aggregate size on concrete resistivity. The results are presented in Section 6 of this white paper.

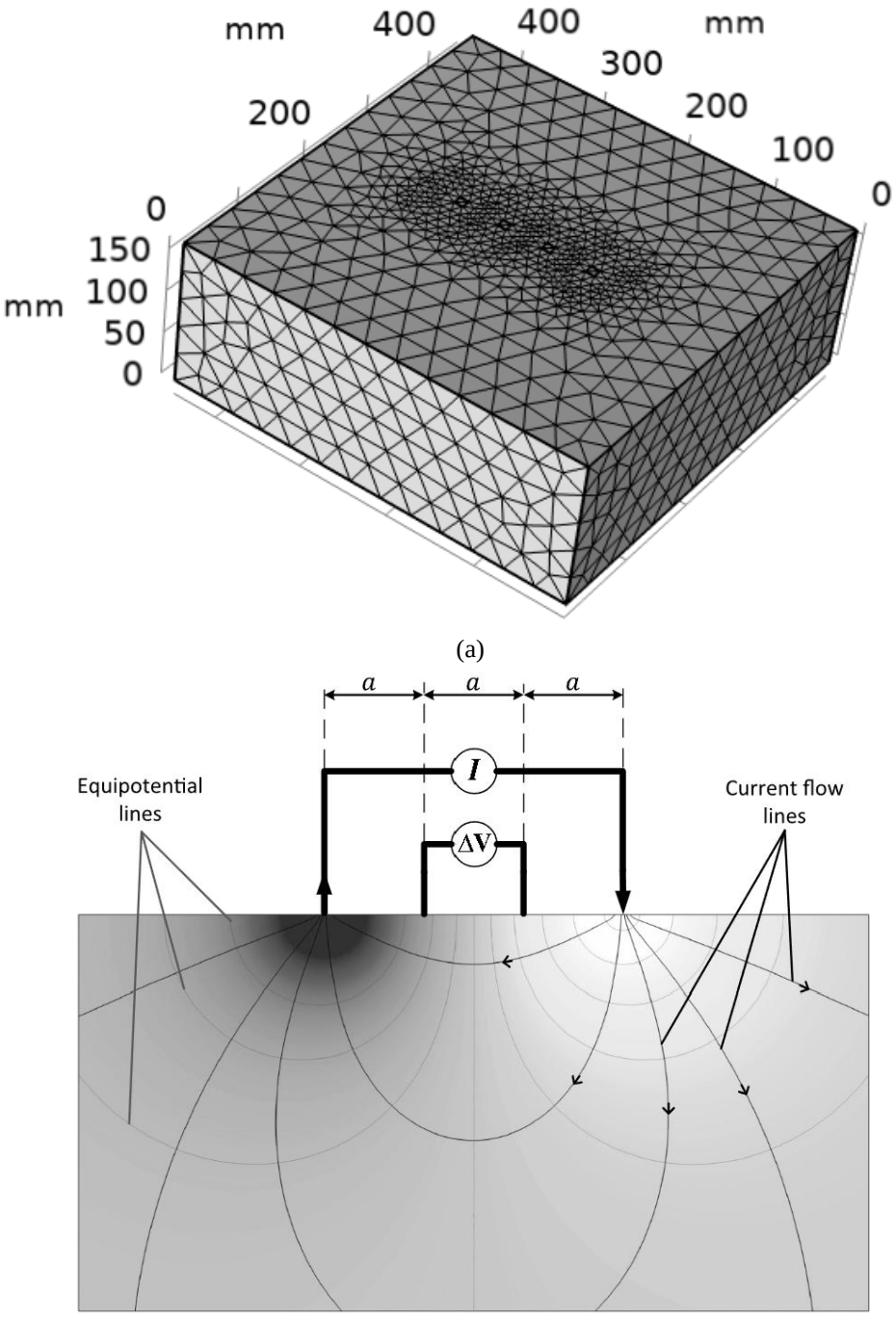

Figure 10. Wenner probe measurement: (a) prismatic discretized domain containing conductive coarse aggregates for surface resistivity simulations using a Wenner probe and (b) cross-sectional view of the Wenner probe measurement process

5.0 ADJUSTING THE SPECIFIED RESISTIVITY FOR CONCRETE WITH CONDUCTIVE AGGREGATE

This section describes an approach in which the measured resistivity of a mortar and its corresponding concrete can be used to determine the aggregate resistivity using equation (11) (equation 4b). The measured resistivity of concrete ($\rho_{concrete}$) and the measured mortar resistivity (ρ_{mortar}) can be used with the resistivity of the conductive aggregate volume (ϕ_A) to determine the resistivity of the aggregate (i.e., $\rho_{aggregate}$).

$$\frac{\rho_{concrete}}{\rho_{mortar}} = \frac{1-\emptyset_A\left[\frac{\frac{\rho_{mortar}}{\rho_{aggregate}}-1}{\frac{\rho_{mortar}}{\rho_{aggregate}}+2}\right]}{1+2\emptyset_A\left[\frac{\frac{\rho_{mortar}}{\rho_{aggregate}}-1}{\frac{\rho_{mortar}}{\rho_{aggregate}}+2}\right]} \tag{11}$$

A series of concretes were prepared in Iowa using limestones with 0.7%, 2.9%, 3.5%, 4.1%, and 6.8% porosity. The resistivities of those concretes were measured to be 10.70, 7.95, 6.05, 6.59, and 4.65 kohm-cm at 28 days, respectively. The mortar from these concretes was measured to have a resistivity of 7.73 kohm-cm. The volume fraction of the aggregate was 33.7%. The aggregate resistivity is shown in Table 1.

Table 1. Computed aggregate resistivity (concrete made with aggregates of varying porosities)

Age (d) 28 day; 33.7% Agg	Mortar	Theory	C-0.7	C-2.9	C-3.5	C-4.1	C-6.8
Concrete Resistivity (kohm-cm)	7.73	13.62	10.70	7.95	6.65	6.59	4.65
Aggregate Resistivity (kohm-cm)	~	inf	25.50	8.41	5.09	4.90	1.71

Figure 11 illustrates the relationship between the resistivity and the porosity of the limestone aggregate, with the fitted relationship shown in equation (12), where C_1 is 0.011 and C_2 is 0.012.

$$\frac{1}{\rho_{aggregate}} = C_1\vartheta^2 + C_2\vartheta \tag{12}$$

where ϑ is the aggregate porosity.

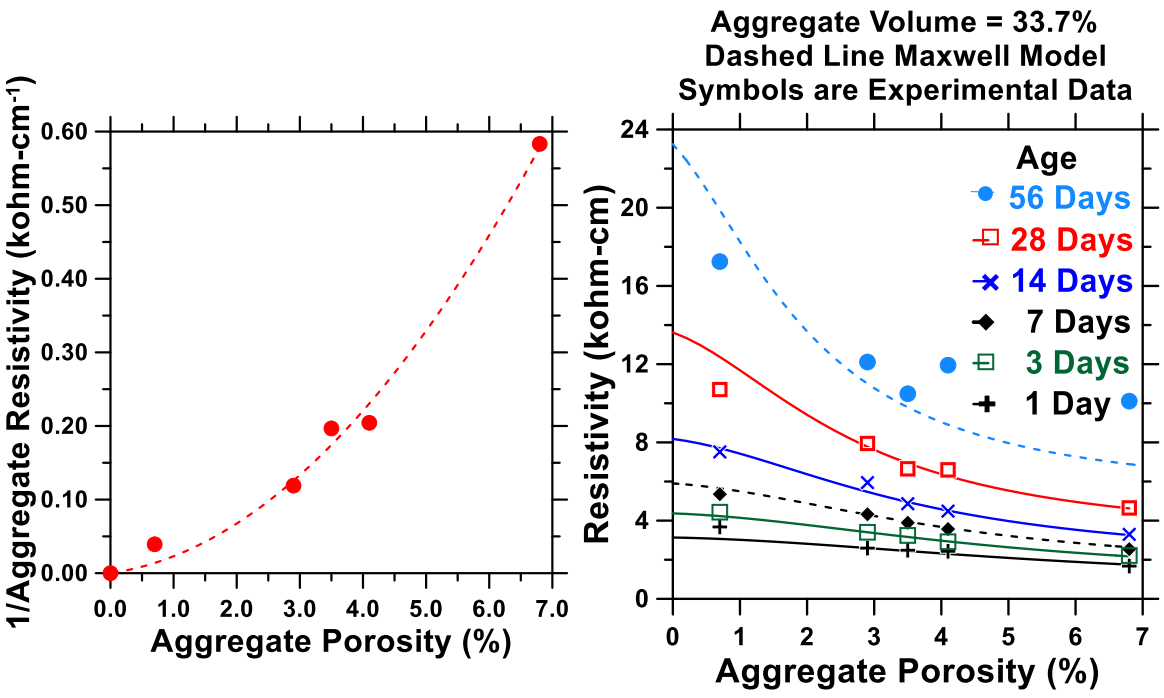

(a) (b)

Figure 11. Comparison of the predicted concrete resistivity using equation (10) and the aggregate resistivity from Table 1: (a) aggregate resistivity versus porosity and (b) concrete resistivity with aggregates of differing porosities

The relationship between the aggregate resistivities and porosity is shown in Figure 11a. The resistivity values of the aggregates obtained from the backfitting procedure (at 28 days) are lower than those measured in the cores (0.25% was approximately 71 kohm-cm and 6.0% was approximately 68 kohm-cm); however, it should be noted that the conditioning procedures and pore solution for the cores were not known. This difference in resistivity values may be expected because the crushing process tends to involve a reduction in the number of large, connected pores because these pores are often the location where fracture planes would occur; crushing thereby converts porosity to surface texture.

Figure 11b provides a comparison of the predicted concrete resistivity values at different ages using equations (11) and (12) based on the aggregate resistivity values from Table 1 (as fitted to the 28-day data). The experimentally measured concrete resistivity values are shown on the plot as well. The values begin to diverge at later ages, which may be due to changes in the aggregate resulting from desorption. However, further examination would be needed to determine the moisture state of the aggregate and the impacts on the measured resistivity. It should be noted that the theoretical resistivity of concrete with infinitely resistive aggregates was calculated to be 13.62 kohm-cm when the aggregate content was 33.7%. This value is very close to the computationally determined concrete resistivity with infinitely resistive aggregates at the same aggregate volume fraction, which is about ~13.1 kohm-cm, as shown in Figure 11a.

The resistivity of a concrete ($\rho_{concrete}$) made with a nonconductive aggregate can be estimated using a mortar matrix with a known resistivity (ρ_{mortar}) and a nonconductive aggregate (i.e., an aggregate with infinite resistivity, $\rho_{aggregate}$), as shown in Figure 12. (Here an aggregate resistivity of 10^8 Ωm is considered sufficiently high to be treated as infinite.) The resistivity of the concrete made with aggregate that is infinitely resistive can be compared to the standard values used in ASTM C1202 to relate the results of the rapid chloride permeability test (RCPT) to electrical resistivity, shown in Table 2. For practical cement clinker-based concretes, there is a lower limit on the results of the RCPT (an upper limit on resistivity) where the conduction is through only the CSH gel (Henkensiefken et al. 2009, Ramanathan 2022). As such, the lowest values on this table appear unachievable.

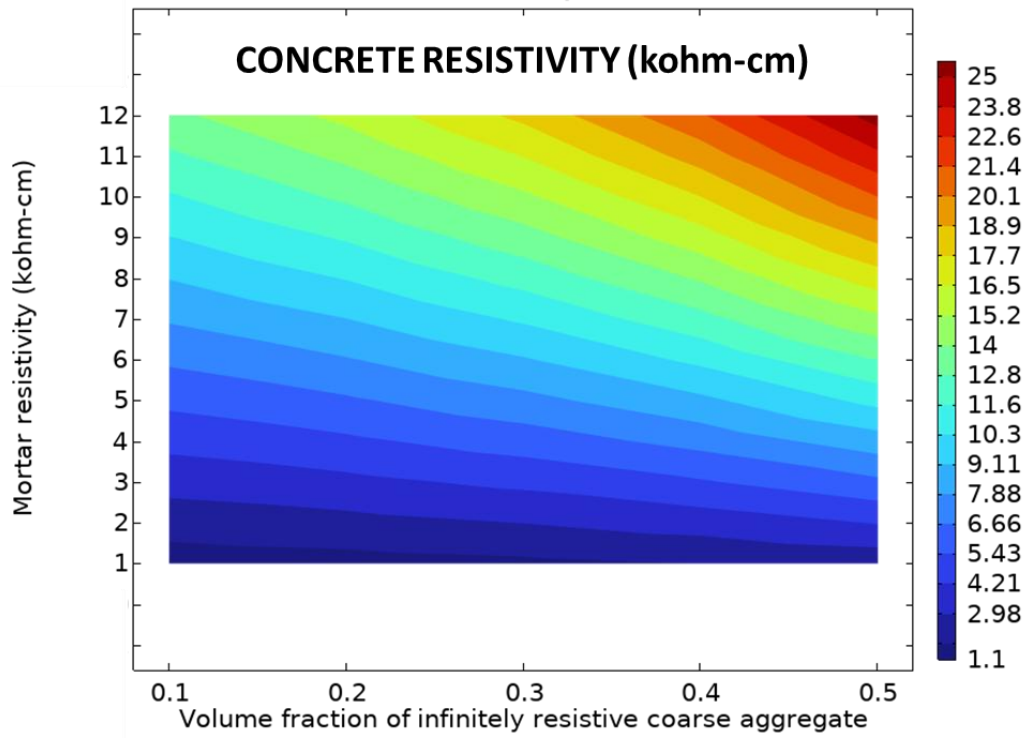

Figure 12. Computed concrete resistivity using infinitely resistive aggregate

Table 2. Relationship between ASTM C1202 RCPT classification and resistivity

ASTM C1202 Classification	Charge Passed (coulombs)		Resistivity of Concrete with Nonconductive Aggregate (kohm-cm)	
High	4000	+	5.2	<
Moderate	2000	4000	10.4	5.2
Low	1000	2000	20.8	10.4
Very Low	100	1000	207	20.8
Negligible	<	100	>	207

6.0 EFFECT OF THE SIZE OF THE COARSE CONDUCTIVE AGGREGATE ON SURFACE RESISTIVITY

As discussed previously, the coarse conductive aggregate size does not appear to have a significant effect on bulk concrete resistivity in the standard configuration, since the current is applied though plates positioned at the top and bottom surfaces of the cylinder that are considerably larger than the maximum aggregate size used in concrete and that create a large sample section to be tested, i.e., 8 inches. (Note, however, that for tests like the RCPT that use smaller sample dimensions, it may be possible for the aggregate to have a measurable effect on bulk concrete resistivity [Spragg et al. 2014].) However, surface resistivity measurements using the Wenner probe may be more sensitive to aggregate size due to the fact that the electrodes have small cross sections and are separated by a limited probe spacing, as shown in Figure 10. The typical probe spacing ranges from 35 mm to 50 mm. Therefore, it is important to develop an understanding of how conductive coarse aggregate size would affect surface resistivity measurements.

Here we simulated several coarse conductive aggregate sizes, assuming a constant volumetric coarse aggregate ratio of 33.7%. The ratio of coarse aggregate resistivity and mortar resistivity was assumed to be 100. For these simulations, where the goal was to investigate the role of aggregate size on the surface resistivity measurements, a uniform coarse aggregate size was used, i.e., the aggregates were not graded. The graded aggregate results could be slightly different from the results of the simulations shown here.

Figure 13 shows the change in concrete resistivity as a function of the ratio of coarse conductive aggregate diameter to probe spacing. A value of 100% indicates that the resistivity measurement is not affected by the conductive coarse aggregate size.

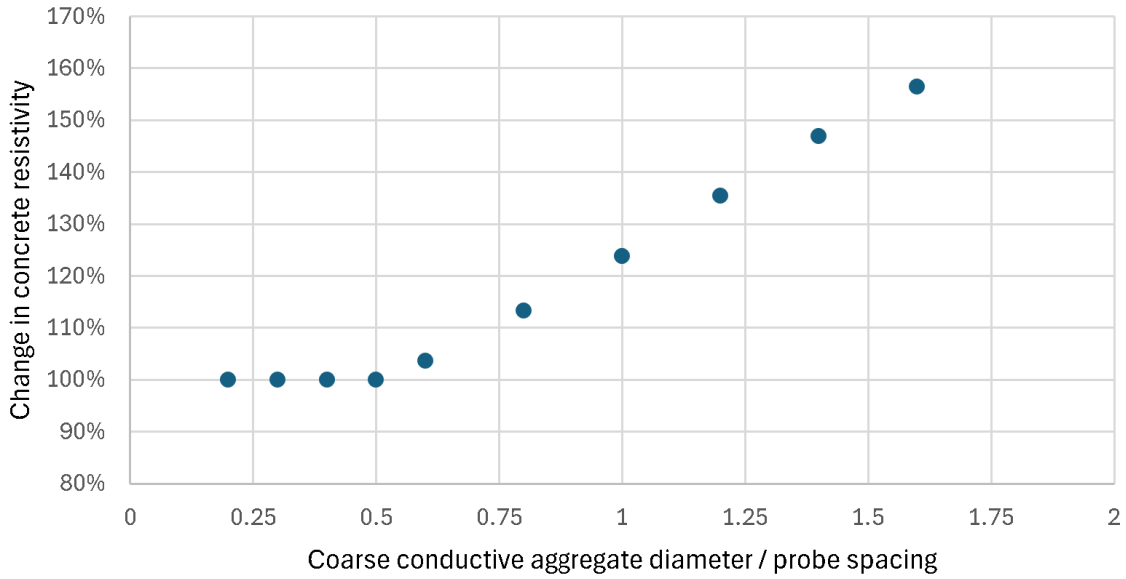

Figure 13. Change in concrete resistivity as a function of the ratio of coarse conductive aggregate diameter to Wenner probe spacing, with 100% indicating that the resistivity measurement is not affected by the conductive coarse aggregate size

The figure shows that the surface resistivity measurements begin to be influenced by the coarse conductive aggregate size after the ratio of coarse conductive aggregate diameter to probe spacing exceeds 0.5. The change in surface resistivity is less than 10% up to a ratio of 0.75 and gets considerably larger as the aggregate size gets closer to and exceeds the probe spacing (~25% when aggregate size = probe spacing; ~50% larger when aggregate size = 1.5 x probe spacing). The calculations imply that when a Wenner probe with a 50 mm probe spacing is used, most of the error associated with the size of the coarse conductive aggregate could be eliminated. When the probe spacing is smaller (e.g., a = 37.5 mm), there would be some error associated with the size of the conductive aggregate, and the level of error would depend on the maximum aggregate size. As a result, for the values typically used (1.5 in. spacing and 1 to 1.5 in. aggregate size according to AASHTO T 358), there would be an influence of geometry that is not present with the uniaxial bulk resistivity.

7.0 SUMMARY, CONCLUSIONS, AND LIMITATIONS

The electrical properties of concrete are used as a surrogate to assess fluid transport in concrete. Some SHAs have reported that the use of certain aggregates tends to reduce the resistivity values of the concrete (all other aspects of the mixture being similar). This white paper examines the role of varying the resistivity of the aggregate using Maxwell's model and a finite element approach. The work provides a procedure to estimate the aggregate resistivity from tests of mortar and concrete samples. If desired, an agency could use this approach to quantify the electrical properties of the matrix phase of a concrete system. Surface resistivity measurements may be sensitive to the aggregate size if the aggregates are conductive. If the ratio of coarse aggregate diameter to probe spacing is less than 0.5, no impact is observed, while for a ratio of

0.75 the increase in surface resistivity is less than 10% and gets considerably larger as the aggregate size approaches and exceeds the probe spacing.

This white paper has not considered the potential for aggregate desorption or the role of the aggregates in changing the interfacial transition zone, which has been examined in earlier work.

8.0 REFERENCES

Aplin, K. L. 2005. Aspirated capacitor measurements of air conductivity and ion mobility spectra. *Review of Scientific Instruments*, Vol. 76, No. 10.

Barrett, T. J., H. Sun, and W. J. Weiss. 2013. *Performance of Portland Limestone Cements: Cements Designed to Be More Sustainable That Include up to 15% Limestone Addition, in Joint Transportation Research Program*. 2013, Indiana Department of Transportation and Purdue University, West Lafayette, IN.

Farnam, Y., H. Todak, R. Spragg, J. Weiss. 2015. Electrical response of mortar with different degrees of saturation and deicing salt solutions during freezing and thawing. *Cement and Concrete Composites*, Vol. 59, pp. 49–59.

Henkensiefken, R., J. Castro, D. Bentz, T. Nantung, and J. Weiss. 2009. Water absorption in internally cured mortar made with water-filled lightweight aggregate. *Cement and Concrete Research*, Vol. 39, No. 10, pp. 883–892.

Munn, R. S., and O. F. Devereux. 1991. Numerical modeling and solution of galvanic corrosion systems: Part 1. Governing differential-equation and electrodic boundary-conditions. *Corrosion*, Vol. 47, No. 8, pp. 612–618.

Rajabipour, F., and J. Weiss. 2006. Electrical conductivity of drying cement paste. *Materials and Structures*, Vol. 40, No. 10, pp. 1143–1160.

Ramanathan, S., K. Bharadway, K. Chopperla, N. Weitzel, O. B. Isgor, T. Van Dam, W. J. Weiss. 2022. *Performance Engineered Concrete Mixtures LTPP Evaluation: Field Performance of Jointed Plain Concrete Pavement Sections in Service; Specific Pavement Studies-2 (SPS-2)*. Oregon State University, Corvallis, WA.

Reynolds, J. M., and J. G. Paren. 1984. Electrical-resistivity of ice from the Antarctic Peninsula, Antarctica. *Journal of Glaciology*, Vol. 30, No. 106, pp. 289–295.

Schießl, A. W. W. Weiss, J. Shane, N. S. Berke, and T. O. Mason. 2000. Assessing the moisture profile of drying concrete using impedance spectroscopy. *Concrete Science and Engineering*, Vol. 2. 106–116.

Shankaramurthy, B. M., K. Wang, and F. Hasiuk. 2021. Influence of carbonate coarse aggregate properties on surface resistivity of high performance concrete. *Construction and Building Materials*, Vol. 312.

Spragg, R., J. Castro, T. Nantung, M. Paredes, and W. Weiss. 2011. Variability analysis of the bulk resistivity measured using concrete cylinders. *Advances in Civil Engineering Materials*, Vol. 21, No. 1. http://dx.doi.org/10.1520/ACEM-2012-0004.

Spragg, R., C. Villani, W. J. Weiss, A. Pourasee, S. Jones, D. P. Bentz, and K. Snyder. 2014. Surface and uniaxial electrical measurements on layered cementitious composites having cylindrical and prismatic geometries. 4th International Conference on the Durability of Concrete Structures, West Lafayette, Indiana, July 2014.

Tarquato, S. 2001. *Random Heterogeneous Materials: Microstructure and Macroscopic Properties*. Springer, Berlin.

Weiss, J., K. Snyder, J. Bullard, and D. Bentz. 2013. Using a saturation function to interpret the electrical properties of partially saturated concrete. *Journal of Materials in Civil Engineering*, Vol. 25, No. 8, pp. 1097–1106.

2711 South Loop Drive, Suite 4700 | Ames, IA 50010-8664 | Phone: 515-294-5798 | cptechcenter.org